SYNTHETIC DOLOMITIZATION : RATE EFFECTS OF VARIABLE MINERALOGY, SURFACE AREA, EXTERNAL CO_3^{2-} AND CRYSTAL SEEDING

By

Timothy R. Bartlett

A THESIS

Submitted to
Michigan State University
in partial fulfillment of the requirements
for the degree of

MASTER OF SCIENCE

Department of Geological Sciences

1984

ABSTRACT

Synthetic Dolomitization:
Rate Effects of Variable Mineralogy
Surface Area, External CO_3^{2-}
and Crystal Seeding

by

Timothy R. Bartlett

The purpose of this study is to evaluate the contributions of several variables on replacement rates during synthetic dolomitization. The specific problem addressed concerns the origin of selective dolomite fabric produced during carbonate diagenesis.

Dolomitization at 175°C resulted in the following order of descending susceptibility to replacement: at equivalent surface areas, aragonite dolomitized more rapidly than Iceland spar calcite, which dolomitized faster than high-magnesian calcite (12 mole % $MgCO_3$). Reaction time generally decreased for finer size reactants (greater surface area). However, an inverse relation between reaction rates and surface area resulted for two calcite samples. The effects of contrasting reactant surface properties on reaction kinetics are invoked to account for this result.

Dolomitization rates were accelerated by the addition of Na_2CO_3 to standard experimental conditions. Seeding reactions with dolomite crystals produced no rate change.

TABLE OF CONTENTS

LIST OF TABLES

LIST OF FIGURES

INTRODUCTION

Dolomitization of $CaCO_3$ in nature can result in certain components of a sediment being selectively replaced while other components remain unaltered. This implies that the rate of dolomitization is not equal for all carbonate reactants within a diagenetic setting. The purpose of this study is to evaluate the influence of several variables on the rate of dolomitization with application to the origin of selective dolomite.

The results of a series of experiments designed to test the effects of 1) reactant mineralogy 2) reactant surface area 3) external CO_3^{2-} and 4) crystal seeding on dolomitization rates are reported and discussed. The underlying assumption is that the more rapidly a reactant is replaced by dolomite in these experiments, the more likely an analogous substrate would be replaced in nature.

Previous Reports of Dolomitization Selectivity

Selective replacement has been attributed to both reactant size and mineralogy. A commonly cited case of selective dolomitization is the replacement of lime mud by dolomite and non-replacement of adjacent allochems and calcite spar (Murray and Lucia, 1967; Schofield and Nelson, 1978; Armstrong et al, 1980). This observation is consistent with the hypothesis that crystal size (surface

area) of the substrate determines its susceptibility to dolomitization.

There are many examples in nature where dolomitization has apparently occurred on a mineralogically selective basis. Kocurko (1979) reported the occurrence where aragonite allochems were dolomitized before high-magnesian calcite (HMC or Mg-calcite, approx. 10-30 mole % $MgCO_3$) and low-magnesian calcite (LMC or calcite, <4 mole % $MgCO_3$). Others have noted that HMC allochems were more readily dolomitized than allochems of LMC (Schlanger, 1957; Schmidt, 1965; Land, 1966; Land and Epstein, 1970; Buchbinder, 1979; Kocurko, 1979; Sibley, 1980 and 1982; and Saller, 1984).

Variations in the rates of $CaCO_3$ replacement during synthetic dolomitization can also be equated to dolomite selectivity. Reactant size and mineralogy may again be important. Mineralogical effects were noted by Gaines (1980), who reported that aragonite dolomitized more rapidly than HMC (30 mole % $MgCO_3$) while dolomitization of LMC was relatively very slow. Studies by Katz and Matthews (1976) and Baker and Kastner (1981) also showed that aragonite dolomitized much faster than calcite.

Dolomitization of Mg-calcites composed of greater than 29 mole % $MgCO_3$ was reported by Land (1967) to have proceeded more rapidly than for aragonite. Mg-calcites having less $MgCO_3$ content were progressively less reactive.

Evidence for crystal size control on dolomitization rates can be found in the work of Bullen (1983). Cryptocrystalline HMC red algae (17 mole % $MgCO_3$), and cryptocrystalline LMC red algae artificially recrystallized from the HMC originals, each dolomitized within equal time intervals. This indicates that the mineralogical difference did not noticably effect the replacement rate. Perhaps dolomitization rates were equal because both reactants had nearly the same surface area, since no textural destruction occurred during conversion of HMC to LMC. Size effects were also apparent in the work of Grethen (1979). His results showed that finely crystalline calcite (approx. 5μm) was replaced in less than one-third of the time required for dolomitization of a coarsely crystalline calcite (75-150μm).

Dolomitization rates may also be influenced by the aCO_3^{2-} and presence of dolomite seed crystals (Morrow, 1982; Lippmann, 1973; Gaines, 1980). Recognition of the rate effects of these variables may therefore provide clues to the origin of selective dolomite.

An abridged summary of the experimental conditions from the cited studies is presented in Table 1. Data has been selected to further illustrate the contrasting reactivities of the carbonate reactants used under the specified sets of conditions. The present study is the first to discriminate the contributions of surface area and mineralogical variation on experimentally determined replacement rates.

Table 1
Previous Experimental Work

Study	Reactant	Grain Size	Ca/Mg (soln)	Conc.	Temp. (°C)	Time for 100% dolo. or % completion
Bullen, (1983)	aragonite pelecypod	3-5 mm fragments, microcrystalline structure	3.13 to 2.33	2M	250	> 247 hrs.
	LMC pelecypod					> 320 hrs.
	LMC echinoid	3-5 mm fragments, cryptocrystalline structure				22 hrs.
	LMC red algae					
	HMC(0.13) foram					92 hrs.
	HMC(0.11) echinoid					
	HMC(0.17) red algae					22 hrs.
Baker and Kastner, (1981)	LMC	powder, 0.51 m^2/g	0.77	I=0.7	200	4.7-6.7 days
	aragonite	no data				< 2 days
Gaines, (1980)	aragonite, seeded	no data	0.20	2M	100	90% in 214 hrs.
	aragonite, unseeded					0% in 214 hrs.
Gaines, (1974)	aragonite	"uniform"	0.25 & 0.20	2M	100	100 hrs.
	HMC(0.32)					400 hrs.
Grethen, (1979)	HMC(0.14)	1-15um crystals	0.14	2M	150	14 days
	calcite	5um rhombs	no Ca^{2+}			≤ 14 days
	calcite	75-150um rhombs				> 14 days
	HMC(0.09) echinoid	75-150um grains	0.20			> 14 < 28 days
	aragonite	1-10um rods				< 8 days
Katz and Matthews, (1976)	calcite	no data	3.8	2M	252	100 hrs.
	aragonite					24 hrs.
Land, (1967)	aragonite coral	skeletal fragments	1.0	0.1M	300	100% in 26 hrs.
	HMC(0.29) red algae					
	HMC(0.11) foram					66% in 26 hrs.
	calcite					29% in 26 hrs.

DOLOMITE SELECTIVITY - THEORY

Selective dolomitization results from contrasting susceptibility to replacement among the variety of carbonate particle types found in nature. Within a particular diagenetic setting, selective replacement by dolomite may be influenced by the mineralogy and crystal size distribution of the pre-dolomitization assemblage. The mineralogy of the reactant will effect the free energy of the reaction, whereas the crystal size of the reactants may effect surface area controlled kinetics of dissolution and/or precipitation.

Potential Thermodynamic Controls on Selective Dolomitization

Reaction 1 is used to demonstrate how differences in reactant mineralogy could cause selective dolomitization. For aragonite reactants x=0, and for calcites, the fraction of Mg^{2+} to Ca^{2+} incorporated in the lattice is substituted for x.

$$2Ca_{1-x}Mg_xCO_3 + (1-2x)Mg^{2+} = CaMg(CO_3)_2 + (1-2x)Ca^{2+} \quad (1)$$

The free energy changes for these reactions in solutions of differing Mg^{2+}/Ca^{2+} are summarized in Table 2. All solutions are supersaturated with dolomite.

Table 2
Thermodynamic Drive of Dolomitization Reactions
ΔG_{dz} = RT ln {K(IAP) / K(eq)}

Environ	Mineral	K_{IAP} [1]	Keq [2]	ΔGdz [3]
Sea Water	HMC(11)[5]	0.248	15.69	-2.46
	HMC(15)	0.286	30.33	-2.76
	Arag	0.167	21.99	-2.89
	LMC	0.167	10.29	-2.44
4 95% F.W. 5% S.W.	HMC(11)	0.794	15.69	-1.77
	HMC(15)	0.813	30.33	-2.14
	Arag	0.743	21.99	-2.01
	LMC	0.743	10.29	-1.56
Laguna Madre Brine	HMC(11)	0.112	15.69	-2.92
	HMC(15)	0.141	30.33	-3.18
	Arag	0.061	21.99	-3.49
	LMC	0.061	10.29	-3.04

1) K_{IAP} for sea water and brine from Gudramovics, 1981; K_{IAP} for mixing zone from Badiozamani, 1973.
2) K_{eq} of mineral + dolomite is calculated from thermodynamic data in Carpenter, 1980; and Morse, 1983.
3) ΔG_{dz} in kcal/mole.
4) 95% fresh water + 5% sea water, from Badiozamani, 1973.
5) HMC(11) and HMC(15) are high-Mg calcites with 11.0 and 15.0 mole % $MgCO_3$, respectively.

The order of decreasing ΔG_{dz} per solution reflects increasing disequilibrium and therefore an increasing potential for dolomite to replace the reactant. Uncertainty in the dolomite and HMC solubility products limits strict application of these calculations; however, both the magnitude and order of decreasing ΔG_{dz} are shown to change as a function of mineralogy and solution chemistry. For example, in the brine solution, the order of increasing $-\Delta G_{dz}$ is: HMC(11) > LMC > HMC(15) > aragonite. Using freshwater-seawater solutions, the order becomes: LMC > HMC(11) > aragonite > HMC(15).

Preferential replacement of one mineral over another suggests a rate effect on the selective process. The association of increasing reactant metastability with potentially rapid reaction rates may thus account for mineralogically selective dolomitization.

Potential Kinetic Controls on Selective Dolomitization

Substrate characteristics that promote dolomite nucleation may effect dolomite selectivity; for example, addition of dolomite seed crystals greatly accelerated the dolomitization rate of aragonite at 100°C relative to unseeded experiments (Gaines, 1980). However, no rate effect was detected in seeded experiments at 295°C by Katz and Matthews (1976). The temperature difference between studies possibly accounts for the conflicting results because nucleation rates increase exponentially

with increasing temperature (Berner, 1980, p. 95, equation 5-15).

Rates of heterogeneous nucleation are also predicted to increase as the degree of lattice similarity between substrate and product becomes greater (Nielsen, 1964, in Berner, 1980). The presence of dolomite seed crystals, at relatively low temperatures, should therefore reduce any lattice-related nucleation barrier to a minimum level and result in accelerated replacement rates. Analogously, selective dolomitization of Mg-calcites over calcite and aragonite substrates may be a result of the closer approximation of the Mg-calcite structure to the dolomite lattice.

The physical nature of a reactant's surface may effect its susceptibility to dolomitization. Steps, kinks and dislocations are features of crystal surfaces which are energetically favored as sites for dissolution and/or heterogeneous nucleation. Relative to planar and unstrained surfaces, enhanced reactivity of such sites can speed surface reations (Berner, 1980; Morse, 1983).

A rapidly dissolving reactant will supply ions to solution faster than a slowly dissolving one. As a result, the ion activity product of dolomite in the bulk solution, and possibly at the interface level, will increase at a relatively greater rate. The sensitivity of nucleation rates to the degree of oversaturation of the precipitating phase (Berner, 1980) could therefore cause

dolomite to nucleate sooner upon the rapidly dissolving substrate.

Dolomite nucleation may also be promoted by the activity of the carbonate ion, independent of the substrate dissolution rate. Beyond its contribution to the IAP of dolomite, CO_3^{2-} ions may enhance the dehydration of Mg^{2+} ions (Lippmann, 1973), thereby increasing the rate of dolomite nucleation and growth. Precipitation experiments by Oomori et al (1983), Nechiporenko and Bondarenko (1984), and Lippmann (1973, Part D) support this hypothesis.

To summarize, a fine grained sediment will expose a greater surface area to a diagenetic solution than an equal mass of a coarser grained sediment and will therefore be favored for dolomitization. Reactants having high densities of reactive sites per unit surface area are also highly susceptible to replacement. Both reactant types will undergo relatively rapid dissolution and provide abundant sites for potential dolomite nucleation.

EXPERIMENTAL DESIGN

A standard set of experimental conditions was employed to determine the time required for complete replacement by dolomite of several calcium carbonate samples (Table 3).

Table 3
Fixed Experimental Conditions

Temperature	175°C
Mg/Ca, solution	4
Ionic strength	3
Sample mass	0.35 g
Solution volume	6.0 ml
Reagents	1M $CaCL_2 \cdot 2H_2O$ plus 1M $MgCl_2 \cdot 6H_2O$

Sample Preparation

Three mineralogies were dolomitized: radial-fibrous aragonite (Ward's Scientific), synthetic aragonite needles, reagent grade calcite (Ward's Scientific and Mallinckrodt), synthetic calcite, optical grade Iceland spar calcite, and biogenic Mg-calcite (echinoderm, 11.8 mole % $MgCO_3$). For the remainder of this paper, the Ward's aragonite, Iceland spar calcite and biogenic Mg-calcite will be referred to as aragonite, calcite and HMC, respectively, unless otherwise stated.

Aragonite, calcite and HMC were manually ground and sieved into 45-75 μm and <45μm size intervals. Multiple decantation with doubly distilled water removed the vast majority of the fine particles produced during crushing and homogenized the grain size distribution of the residuum. These suspensions were then retained as samples, with crystal diameters in the 1-10μm range. Organic matter within the echinoderm skeleton was removed by soaking fragments in a Chlorox solution for 24 hours,

followed by thorough rinsing. All crushed samples (aragonite, calcite and HMC) were oven dried for 24 hours at about 75°C after decantation and rinsing.

Surface Area

Surface area of all samples were calculated by application of the BET equation (see Adamson, A.W., 1982, Chap. XVI) to nitrogen adsorption data obtained from the Perkin-Elmer Model 212B "Sorptometer". Results of the surface area determinations appear in Table 4a. The range of surface areas obtained was between 2.66 and 0.15 m^2/g, corresponding to average crystal diameters of about 5µm and 75µm, respectively. The average percent difference for all samples run more than once is equal to ±8.2%; the average absolute difference for the same runs equals ±0.107 square meters per gram.

Several estimates of geometric surface area from microscopic examination are listed in Table 4b. The calculations are based on assuming cylindrical shapes for sample AF2 (aragonite needles), and cubes for samples CI3 and CF2 (equant calcite rhombs). The consistency of the geometric to BET ratios suggests internal consistency of adsorption data and surface area calculations.

Dolomitization Method

Approximately one-hundred experiments were run to test for surface area and mineralogical influences on

Table 4a
BET Surface Area (SA) Results

Mineral	SA, m^2/g	# runs	Source	Symbol
Aragonite				
coarse	0.17 ± 0.017	2	Ward's Sci.	AC
intermediate	1.06	2	"	AI
intermediate	0.29	1	"	AI2
fine	1.2 ± 0.015	2	"	AF
fine	1.8 ± 0.22	3	synthetic	AF2
HMC				
coarse	0.54	1	echinoderm	HC
intermediate	0.79	1	"	HI
fine	1.85 ± 0.05	2	"	HF
Calcite				
coarse	0.15	1	Iceland spar	CC
intermediate	0.73	1	"	CI
intermediate	0.25	1	reagent	CI2
intermediate	0.59 ± 0.075	2	synthetic	CI3
fine	2.66 ± 0.045	2	Iceland spar	CF
fine	1.87 ± 0.34	3	reagent	CF2

Average absolute difference equals ± 0.107 m^2/g for all multiply run samples, average % difference equals ±8.2%

Table 4b
Geometric Comparison to BET Surface Areas

Sample	Geometric Estimation, m^2/g	Geometric/BET
AF2	8.5	4.7
CI3	2.52	4.3
CF2	7.5	4.0

dolomitization rates. The dolomitization method consisted of placing a known mass of a sample, plus solution, into stainless steel Stellate-type bombs. These were placed into a muffle furnace set at 175°C. Numerous runs were performed for each sample and many were quenched at various intervals prior to 100% dolomitization. In this way, the effect of surface area variation on the rate of replacement could be ascertained per mineral; and, at a given surface area, the relative effect of reactant mineralogy on the replacement rates could be directly compared.

In addition, twenty-one experiments were run to determine the effects of 1) an external source of the carbonate ion and 2) seeding experiments with dolomite. The affect of external CO_3^{2-} was determined by adding 10 weight % (of the sample mass) Na_2CO_3 to normal starting conditions just prior to bomb sealing. This amount was sufficient to cause initial supersaturation with calcite; however, no precipitate was observed from the bomb solution within twenty minutes after Na_2CO_3 addition at room temperature and pressure. Several experiments seeded with synthetic dolomite (5 weight % of the sample mass) produced during previous runs were also run alongside the external CO_3^{2-} runs. Seeds consisted of both disordered and well-ordered dolomite. Control runs lacking Na_2CO_3 and seeds were run simultaneously with the other runs.

Analyses

X-ray diffraction analyses for phase identification, composition and ordering (Graf and Goldsmith, 1956; Gaines, 1974) were made after bomb quenching, product filtration, rinsing and air drying. Detailed petrographic descriptions are included in Appendix 1. Reactants and products were examined with an SEM.

Percent dolomite was estimated petrographically with the aid of Alizaren red-S staining. This method was practical among the coarser grained reactants when dolomite appeared to be sparsely distributed on reactant surfaces. Dolomite content was also estimated by comparing product diffractograms to prepared calibration curves, where dolomite to reactant peak height ratios were plotted against their known weight proportions. This method was employed among the finer grained reactants and when the dolomite content visually exceeded about 10-20 percent.

RESULTS

Reaction Sequence

Plots of percent dolomite with respect to time, per mineral and surface area category, are presented in Figures 1-6. The form of these plots is similar among the different reactants. Each figure consists of points

located along the x-axis representing runs containing no dolomite, followed in time by an abrupt change to points which correspond to runs containing 100% dolomite. Few points appear in intermediate positions. The lines in Figures 1-6 were hand drawn for schematic purposes only.

Microscopic and X-ray diffraction analyses revealed that two distinct reaction stages accounted for the characteristic shape: 1) partial reactant dissolution and precipitation of intermediate phases occurred in the runs located on the x-axis, and 2) dolomite precipitation and accelerated reactant dissolution occurred in the interval between the last point on the x-axis and the first appearance of 100% dolomite.

Partial dissolution and intermediate phases

A small amount of substrate dissolution occurred preceding the crystallization of intermediate phases. Further reactant dissolution followed.

Figures 7-12 typify the occurrence of intermediate phases and partial grain dissolution during the pre-dolomite stage of the reaction sequence. Calcite dissolution is marked by distinct lattice related etch features and retention of sharp edges (Figure 7, compare with unreacted Iceland spar calcite, Figure 8). Dissolution of aragonite however produced rounded corners and surface pits (Figure 9, compare to Figure 10, unreacted

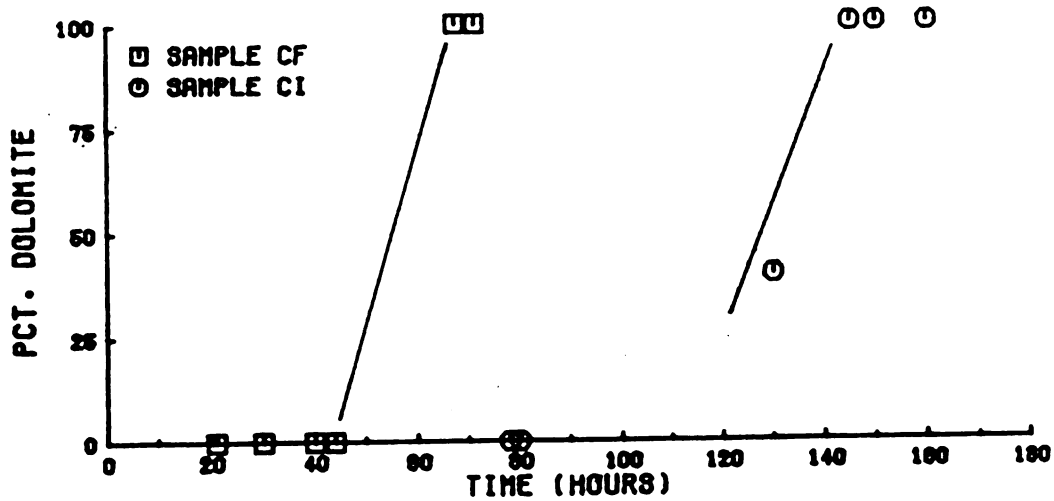

Figure 1a

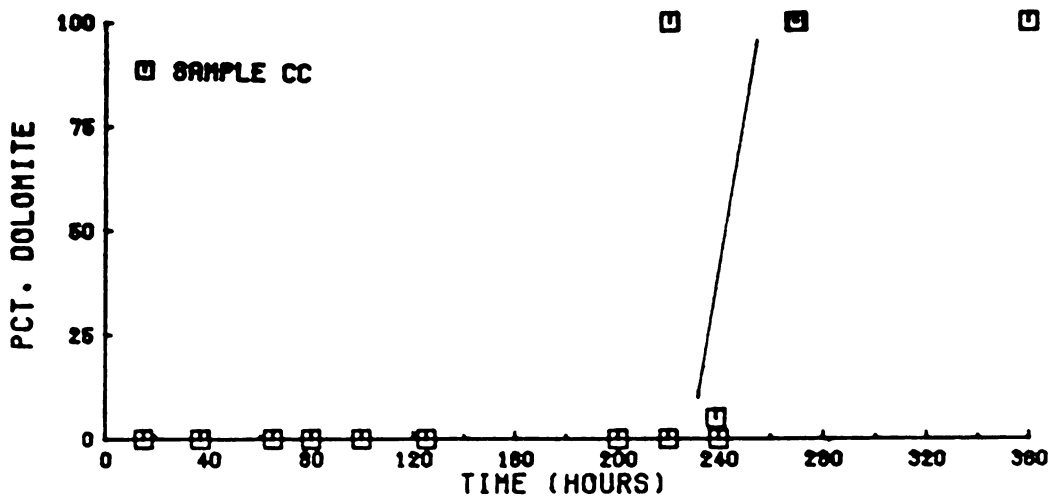

Figure 1b

Figure 1
Iceland Spar Calcite

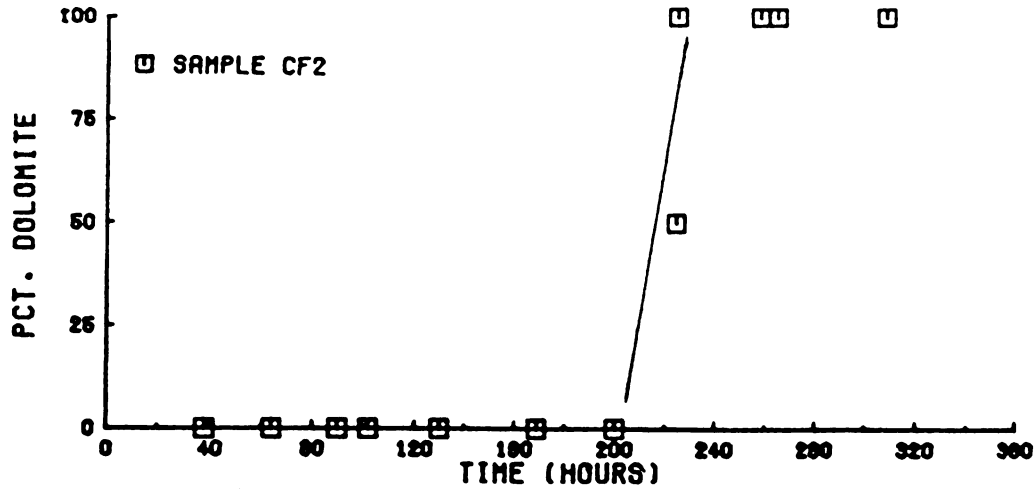

Figure 2a

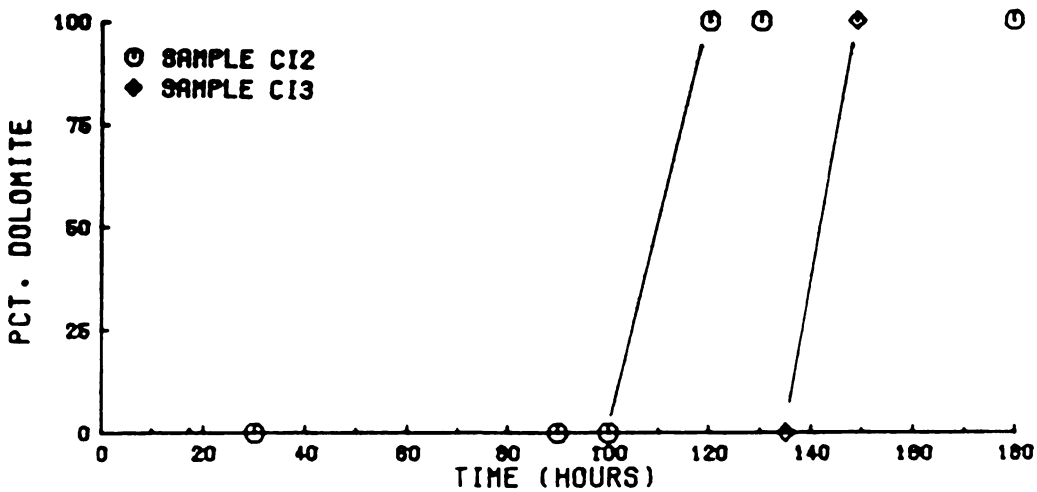

Figure 2b

Figure 2
Synthetic Calcite

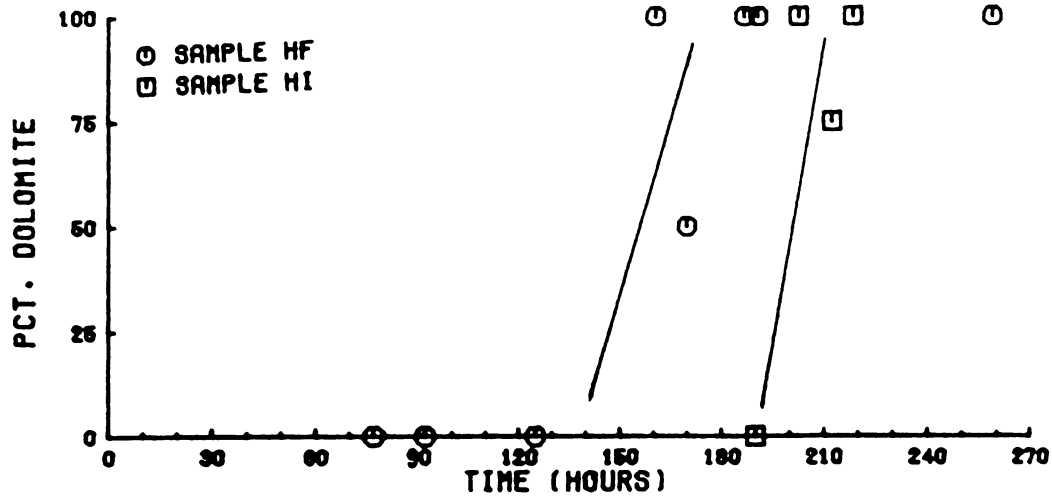

Figure 3a

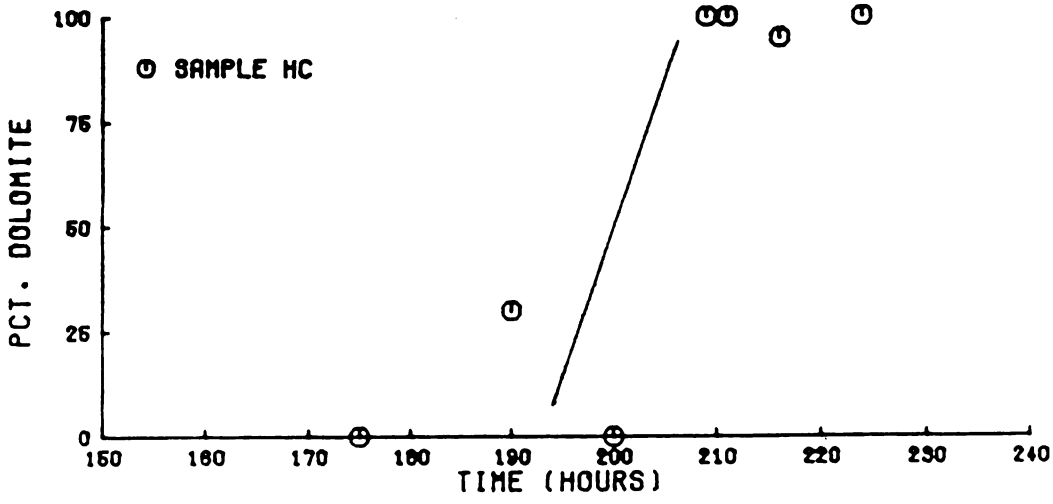

Figure 3b

Figure 3
HMC

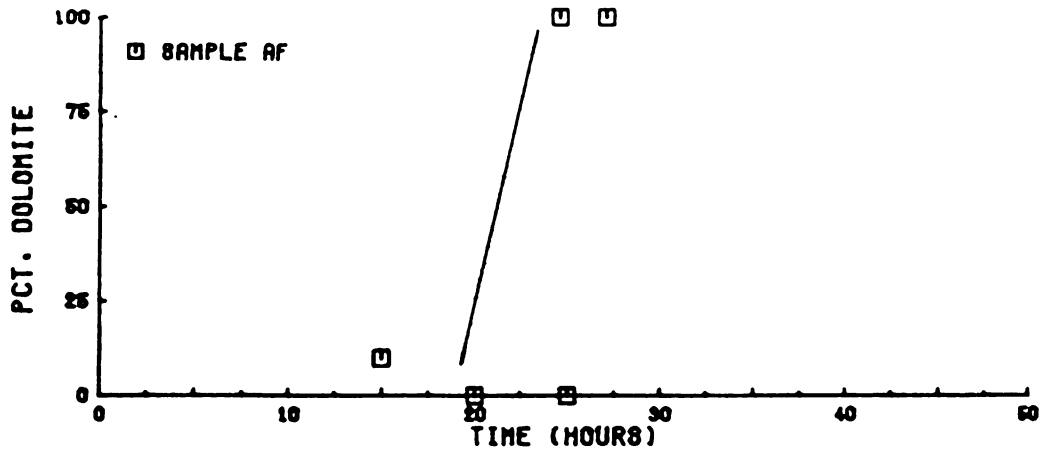

Figure 4a

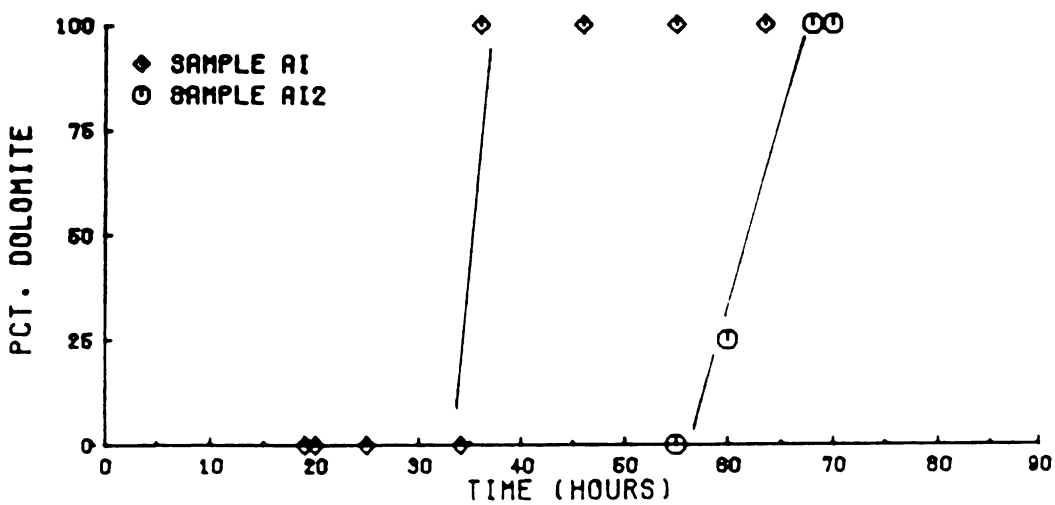

Figure 4b

Figure 4
Ward's Aragonite

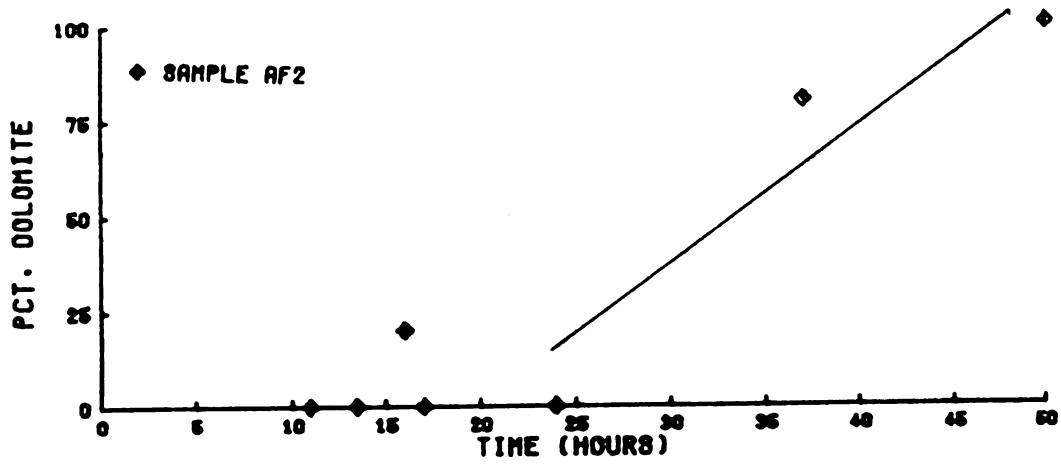

Figure 5a
Synthetic Aragonite Needles

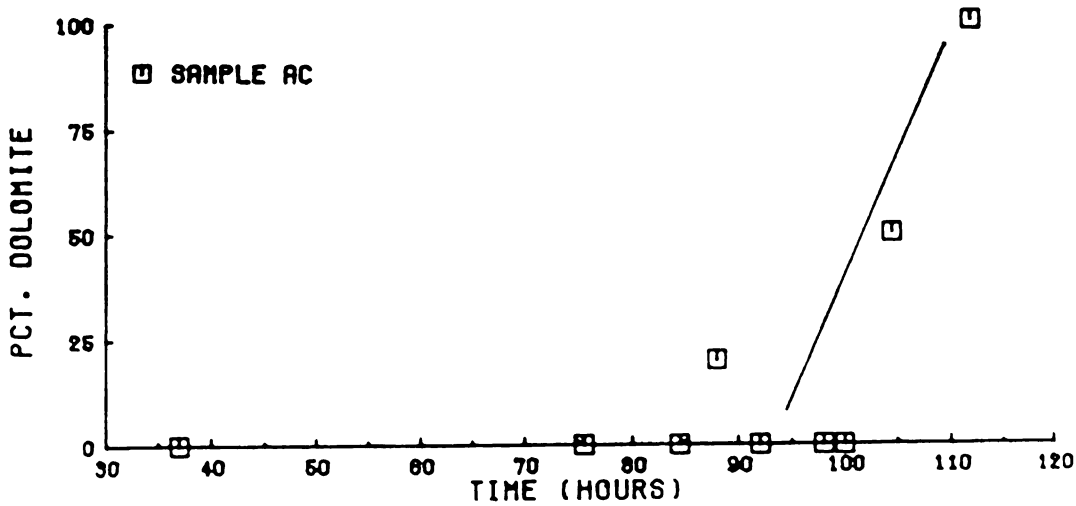

Figure 5b
Ward's Aragonite

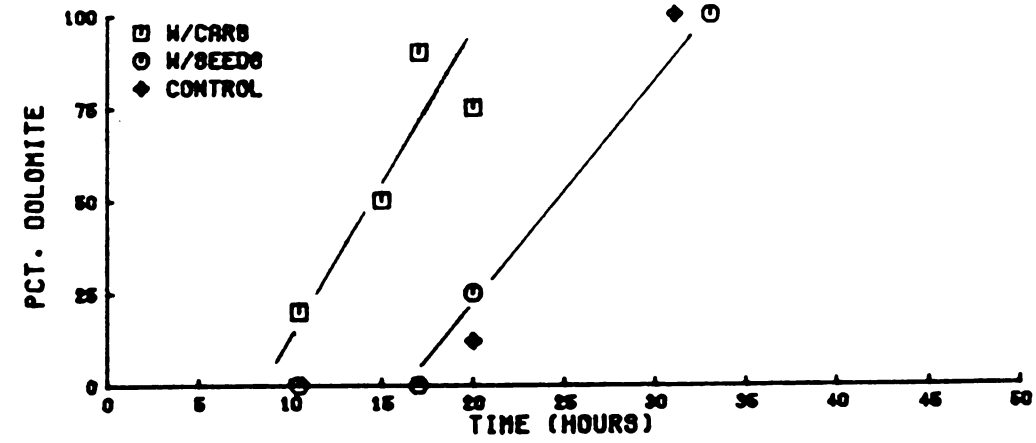

Figure 6a
Sample AI

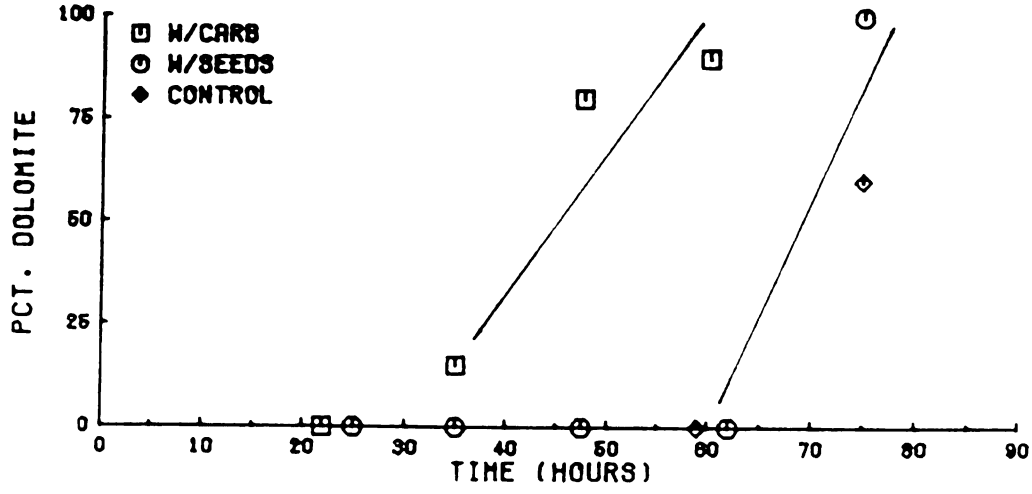

Figure 6b
Sample CF'

Figure 6
External Carbonate and Seeds

Ward's aragonite). HMC dissolution occurred preferentially within certain regions of the grains to form internal voids (Figure 11, see Figure 12 for unreacted HMC). Inner surfaces of these features appeared ragged while the outer surfaces remained smooth and apparently non-etched.

Aragonite dissolved more rapidly than calcite and HMC. The rate of HMC dissolution was the slowest among these reactants. Abundant etch pits were observed on aragonite (sample AC) after 37 hours of reaction. Over the same amount of time, calcite of comparable surface area (sample CC) had no etch features. Fine grained HMC (sample HF) showed no evidence of dissolution within 92 hours, whereas a coarser grained calcite (sample CI) was strongly etched within 80 hours. There was never an example of total dissolution of a primary substrate before dolomite appeared.

The composition and mineralogy of the intermediates which precipitated varied with the reactant. Magnesite precipitated during LMC runs, ranging in composition between 6 and 15 mole % $CaCO_3$ (identification and composition determined by the presence and location of the (104) peak; Grethen, 1979). The compositional range of magnesite formed in HMC runs was 9.4 to 12 mole % $CaCO_3$.

The earliest magnesite crystals were sometimes observed to have formed preferentially along calcite twin planes; otherwise, a preferred orientation did not result. Individual crystal sizes ranged between 1 and 10µm,

Figure 7 Early dissolution of Iceland spar calcite. Grains are angular and show lattice-like etch features. 1000X, scale bar equals 20µm.

Figure 8 Unreacted Iceland spar calcite. 700X, scale bar equals 28.6µm.

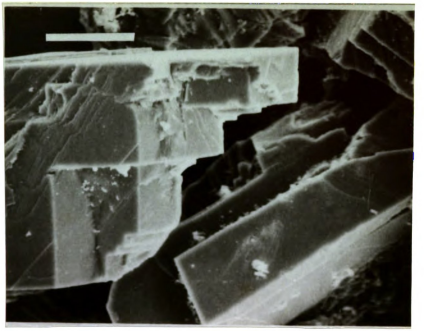

Figure 7

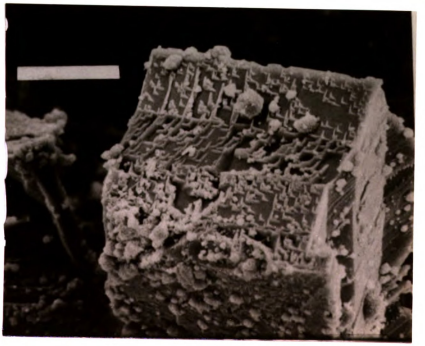

Figure 8

Figure 9 Dissolution etching of Ward's aragonite. Note the rounded corners and surface pits. 2000X, scale bar equals 10μm.

Figure 10 Unreacted Ward's aragonite, radial-fibrous texture is displayed. 2000X, scale bar equals 10μm.

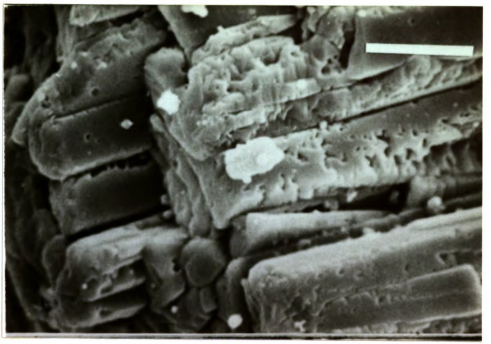

Figure 9

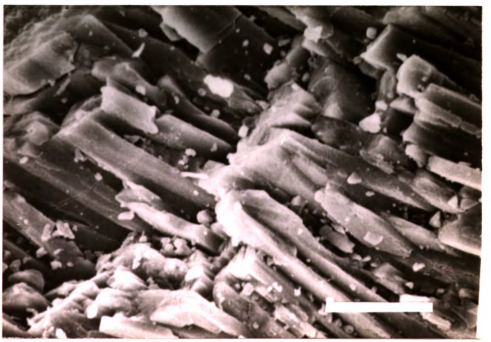

Figure 10

Figure 11 Partially dissolved Mg-calcite. Regions of preferential dissolution are indicated by the arrows. Bright colored material is magnesite. 3000X, scale bar equals 6.7μm.

Figure 12 Unreacted HMC echinoid grains. Bright material is fine grained HMC adherred to large grain surfaces. 400X, scale bar equals 50μm.

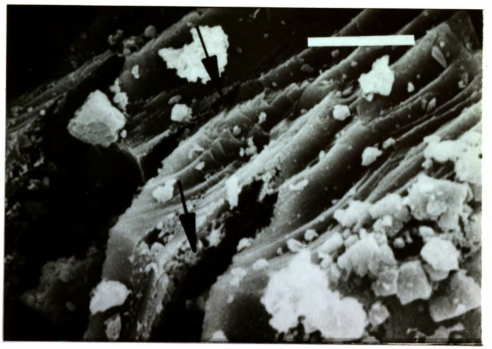

Figure 11

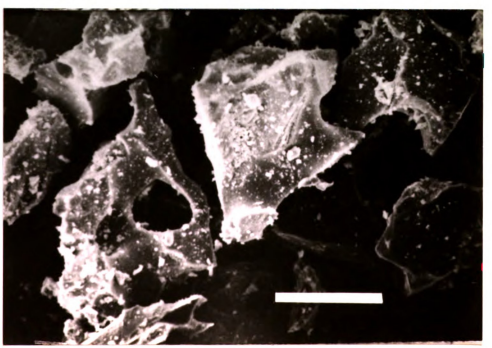

Figure 12

occurring as subhedral rhombs with highly stepped surfaces. Magnesite packing on substrate grains from a single run varied from dense coverings to nearly barren surfaces. The total content never exceeded approximately 5-10% of total solids present. Magnesite appears in Figs. 7 and 11 as the lighter toned, randomly distributed subhedral crystals.

Experiments with aragonite reactants did not produce magnesite. Instead, an amorphous material formed during the Ward's aragonite runs, and HMC (15 mole % $MgCO_3$) formed during runs using synthetic aragonite needles. Crystals of the HMC intermediate displayed a euhedral prismatic habit and attained long dimensions of 10-15μm, substantially coarser than the reactant needles (2-5μm in length). The amorphous material appeared as clustered spherulites with diameters of approximately 2-5μm.

Interval of dolomite precipitation

The second stage in the reaction sequence involved dolomite precipitation and accelerated substrate dissolution. The abrupt change from 0% to 100% dolomite in Figures 1-6 indicates that precipitation of dolomite proceeded rapidly once initiated. The time span between the first appearance of dolomite and 100% replacement was commonly about 15 to 20 hours, which is in general, much shorter than the partial dissolution stage. Coarse grained HMC, for example, dolomitized in the interval between

190 and 210 hours (Figure 3b).

Figures 13 and 14 show the distribution of early, minute dolomite crystals (0.25-5μm) on HMC and calcite hosts, respectively. Dolomite is distinguished from magnesite in the SEM images by its euhedral form and strong preferential alignment. Nucleation of dolomite on aragonite produced a non-preferentially aligned fabric (Figure 15). In all experiments, the dolomite nucleated directly on the primary substrate surface rather than upon intermediate phases.

Compositions of dolomite detected prior to 100% replacement of the reactant are listed in Table 5. All such occurrences were Ca-rich relative to ideal dolomite; however, a uniform composition common to each reactant mineralogy did not result. Instead, a distinct compositional range characterized each reactant (see Table 5). Reproducibility of the compositions from X-ray diffraction equals 1.2 mole % $CaCO_3$. The dolomite was either poorly-ordered or disordered at this point in the reaction.

Table 5
Dolomite Compositions Prior to 100% Dolomitization

Reactant	Average composition (mole % $CaCO_3$)	No. runs
HMC	52.3	4
Calcite	55.2	8
Aragonite	61.5	11

Figure 13 Earliest dolomite detected on HMC substrate. The dolomite is euhedral and shows a strong preferential alignment. Other crystals are magnesite. The finest crystals of dolomite are about 0.25μm in diameter. 5000X, scale bar equals 4μm.

Figure 14 Earliest dolomite on Iceland spar calcite. The dolomite shows a strong preferred orientation and forms directly on the calcite surface (Fig. 13 also). Note the rounded corners of the substrate. 3000X, scale bar equals 6.7μm.

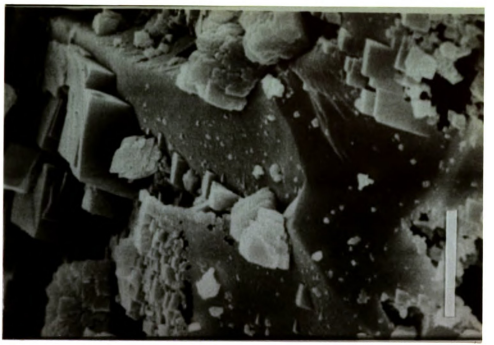

Figure 13

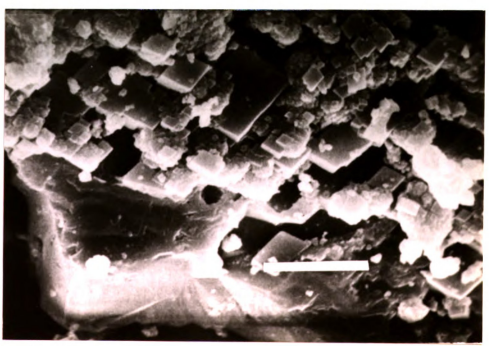

Figure 14

Figure 15 Early dolomite rhombs on Ward's aragonite. The dolomite is euhedral and randomly oriented. 7000X, scale bar equals 2.9μm.

Figure 16 Edge and corner dissolution rounding on Iceland spar calcite at the onset of dolomite precipitation. 1000X, scale bar equals 20μm.

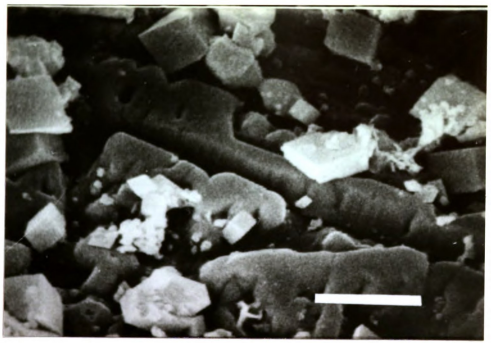

Figure 15

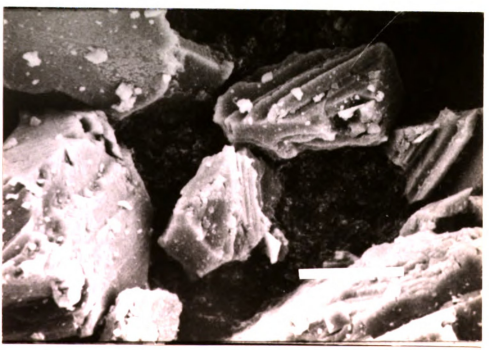

Figure 16

Concurrent with rapid crystallization of dolomite was rapid substrate dissolution, i.e., substrate dissolution rates were accelerated during the dolomite precipitation stage. Calcite grains became distinctly rounded, in contrast to the sharp edges and corners produced during the earlier pre-dolomite stage (refer to Figs. 14 and 16). Aragonite and HMC dissolution textures remained unchanged.

Magnesite dissolution was completed before LMC was entirely replaced by dolomite. However, it persisted during HMC runs for approximately 100 hours after all HMC had been dolomitized. HMC produced during synthetic aragonite runs existed with dolomite for about 24 hours after the aragonite had been completely replaced.

Figures 17-20 are SEM images showing representative textures of final dolomite products. Replacement of individual crystals of coarse calcite and HMC resulted in highly oriented polycrystalline dolomite grains (Figs. 17 and 18). The dolomite preserved only a crude outline of the primary grain. Dolomite replaced HMC to produce rhombic shaped grains, despite originally anhedral shapes. Non-undulatory unit extinction was exhibited by the polycrystalline grains. Coarsely crystalline aragonite was replaced by randomly oriented dolomite rhombs. Virtually no precursor texture was preserved by the resulting interlocking mosaics (Figure 19).

Finely crystalline reactants tended to be replaced by individual dolomite rhombs. Figure 20 exemplifies the

Figure 17 Final dolomite texture after Iceland spar calcite. The oriented crystals produce unit extinction of entire grains under crossed polars. 700X, scale bar equals 28.6μm.

Figure 18 Final dolomite texture after HMC. Grains have taken on rhombic shapes, contrasting with originally anhedral shapes. These grains typically show unit extinction under crossed polars. 1000X, scale bar equals 20μm.

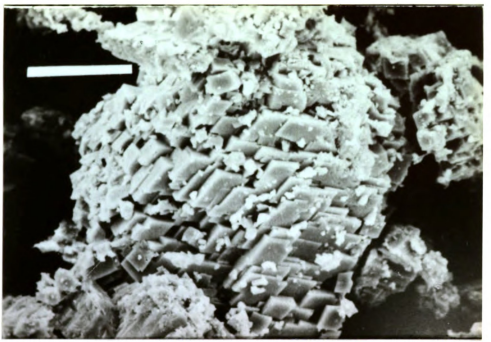

Figure 17

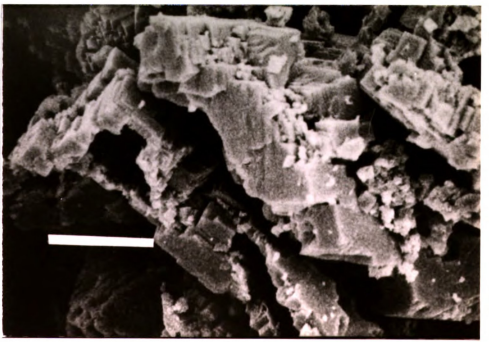

Figure 18

Figure 19 Final dolomite texture after Ward's aragonite. Random orientation of the dolomite rhombs has totally destroyed the primary aragonite texture. A remnant of the reactant appears in the lower right corner. 1000X, scale bar equals 20μm.

Figure 20 Final dolomite texture after a reagent calcite. Single crystal replacement contrasts to the polycrystalline product of Figs. 18 and 19. 3000X, scale bar equals 6.7μm.

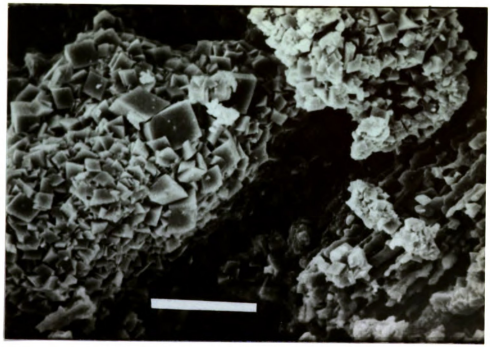

Figure 19

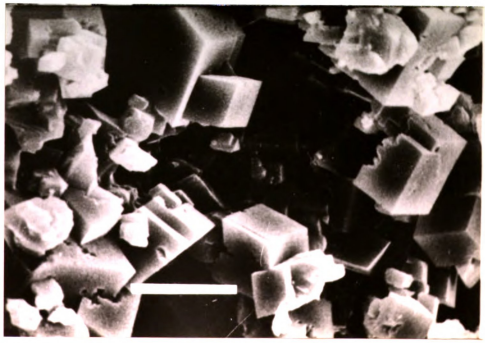

Figure 20

replacement dolomite texture after a reagent calcite powder (Sample CF2). Dolomitization of fine grained reactants also appeared to produce a slight grain coarsening.

Ordering of the dolomite product was assigned on a relative scale based on the position and definition of the (006) and (015) superstructure peaks. Dolomite progressed with reaction time from an initially disordered phase to a well-ordered final product, achieving its maximum degree of ordering within approximately 25 hours after it was first detected. The final products of this study, however, never displayed superstructure peaks equal in intensity and definition to those of ancient dolomite samples.

Dolomite composition progressed from an early Ca-rich phase (Table 5) to a nearly stoichiometric final product. This change occurred within the interval between the first detection of dolomite and the earliest occurrence of 100% dolomite for that reactant. No trend in compositional variation was observed beyond this point. The final dolomite composition for each mineralogy was quite uniform. The average final dolomite composition for HMC was 52.2 mole % $CaCO_3$, for calcite, 51.3 mole % $CaCO_3$, and for aragonite, 51.7 mole % $CaCO_3$.

Surface Area vs. Time for 100% Dolomitization

Figure 21 is a plot of surface area (Table 3a) versus the minimum time required for complete dolomitization (from Figures 1-6). Negative slopes of the HMC, calcite and

aragonite curves imply that with increasing substrate surface area, less time was required for dolomitization. Synthetic calcites reacted oppositely, i.e., complete replacement of the high surface area calcite required the most time and vice versa (positive slope, Fig. 21). The reaction time for synthetic aragonite needles also did not plot on the Ward's aragonite curve, requiring as much time to dolomitize as a substantially coarser Ward's sample.

Seeding and External Carbonate Ion

Samples CF and AI were used to compare the effects of dolomite crystal seeding and addition of Na_2CO_3 on the rates of dolomitization. The sequence of reaction events during these experiments replicated those described above for calcite and aragonite reactants. SEM indicated however that dissolution of the substrate was more pronounced in the seeded runs than external CO_3^{2-} runs over equal periods of time.

Seeding did not noticably accelerate the reaction rate relative to control runs for either calcite or aragonite reactants (Fig. 6). Addition of Na_2CO_3 did however result in significantly accelerated rates (Fig. 6). The first appearance of dolomite was always detected much sooner in these runs, resulting in a reduction in the total time for replacement by about one-third.

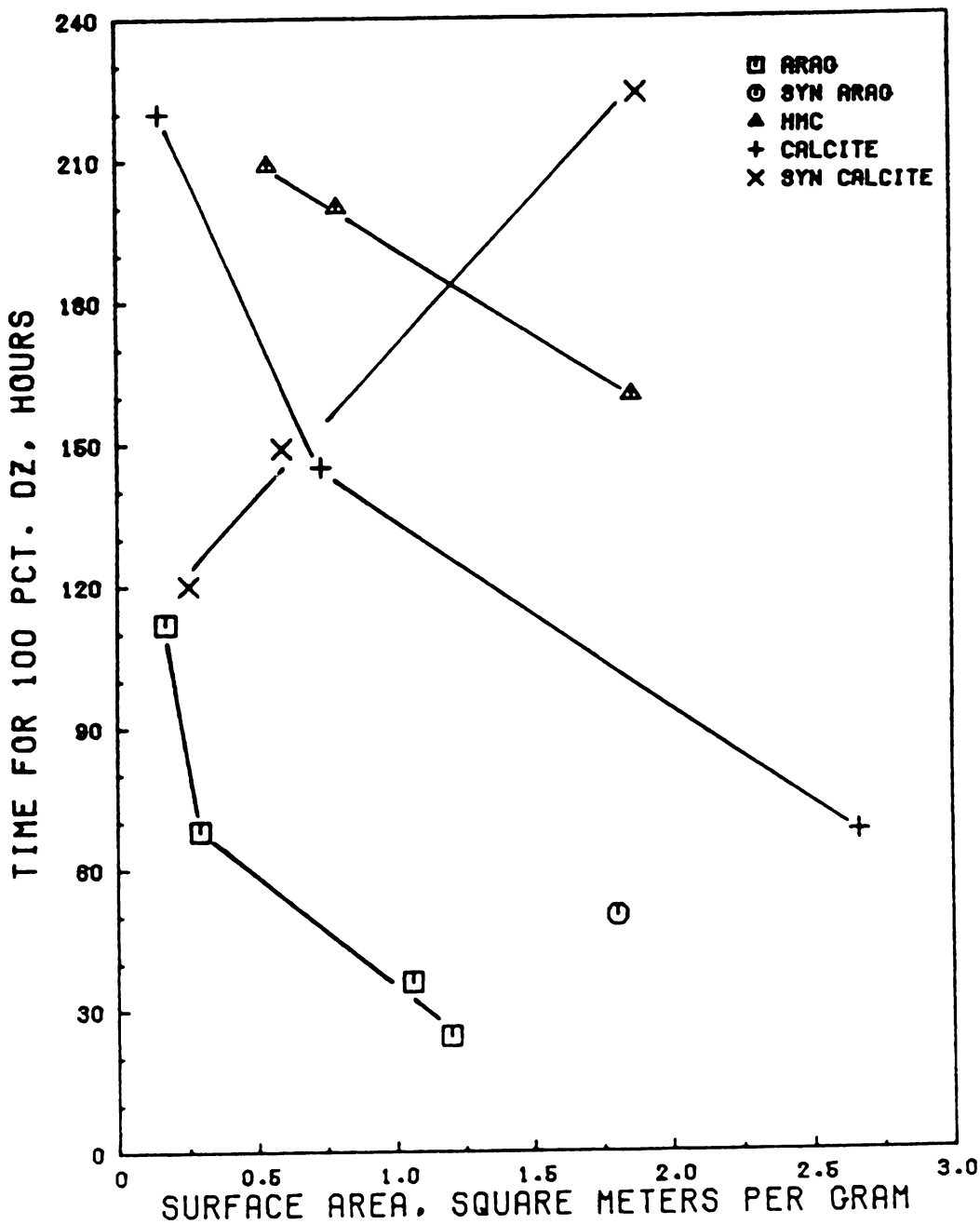

Figure 21
Minimun Time for 100% Dolomitization vs.
Reactant Surface Area

INTERPRETATION AND DISCUSSION OF EXPERIMENTAL RESULTS

An examination of Fig. 21 suggests that mineralogy is more important than surface area in determining the relative susceptibility to dolomitization between the aragonite, calcite and HMC reactants. The vertical separation between reactant curves typically accounts for more reaction time than is represented by the rise of the slope along an individual reactant curve. Superpositioning of these curves does not occur, nor do they intersect within the range of surface areas tested; such would be expected results if crystal size were hypothesized as the stronger rate determining variable.

Surface area variation is obviously important per mineral however, because the curves for aragonite, Iceland spar calcite and HMC each slope negatively. Non-intersection of these curves for all surface areas, indicates that aragonite dolomitized more rapidly than Iceland spar calcite, which in turn dolomitized faster than HMC (12 mole % $MgCO_3$).

Neither mineralogy nor surface area emerged as the dominant rate controlling variable however. The coarse grained Iceland spar calcite and coarse synthetic calcite dolomitized at very different rates, although they were of identical composition and had approximately equal surface

areas. A strict mineralogical control did not therefore have a consistent effect on replacement rates. Furthermore, the oppositely sloping curve of the synthetic calcites (Fig. 21) indicates that surface area variation did not have a consistent effect on the replacement rates either. The following two sections address the processes that were recognized during dolomitization and their possible roles in determining reaction rates.

Nucleation of Dolomite

Dolomite seeding had no apparent effect on reaction rates. In addition, the earliest nucleation of dolomite was detected on an aragonite substrate although its lattice structure is least similar to that of dolomite among the reactants tested. Nucleation of dolomite occurred latest on the HMC of equivalent surface area. Therefore, relative nucleation rates were not influenced by the lattice similarity between the substrate and dolomite. These results tend to support the hydration barrier hypothesis proposed by Lippmann (1973) as an obstacle to crystallization.

The strong preferential alignment of dolomite crystallites on HMC and calcite, but random orientation on aragonite, suggest that the lattice similarity between substrate and dolomite determined the nucleation fabric. The fabric of the final product was subsequently controlled by that of the earliest crystals (refer to Figs. 18-20).

The observed order of dolomite nucleation rates may have been determined by the relative rates of substrate dissolution. Since CO_3^{2-} was derived solely from the reactant in the standard experimental runs, the aCO_3^{2-} and saturation state of dolomite would be directly effected by the dissolution rate. These factors should have consequently influenced the rate of dolomite nucleation. By this mechanism, nucleation occurred sooner upon aragonite than other reactants because of the greater rates of CO_3^{2-} production and increasing IAP of dolomite, via rapid dissolution. Results of the Na_2CO_3 runs support this interpretation.

Dolomitization was accelerated by the addition of Na_2CO_3. However, immediate nucleation did not occur and etching of calcite was observed prior to the detection of dolomite. The rate increase in the Na_2CO_3 runs may have occurred because 1) the substrate dissolution step was eliminated as the single source of CO_3^{2-} and 2) dolomite oversaturation was greater relative to standard runs.

The inverse relation between surface area and dolomitization rates of the synthetic calcites (Fig. 21) is attributed to the effects of surface properties on dissolution and nucleation rates. SEM revealed the surfaces of the fine grained synthetic calcite to be extremely smooth and perfect (Fig. 22). By contrast, the more reactive but coarser grained sample had imperfect,

Figure 22 Sample CF2. Rhomb surfaces appear extremely smooth even at high magnification. 10,000X, scale bar equals 2μm.

Figure 23 Sample CI2. Crystal surfaces are stepped and non-uniform relative to Sample CF2. 3000X, scale bar equals 6.7μm.

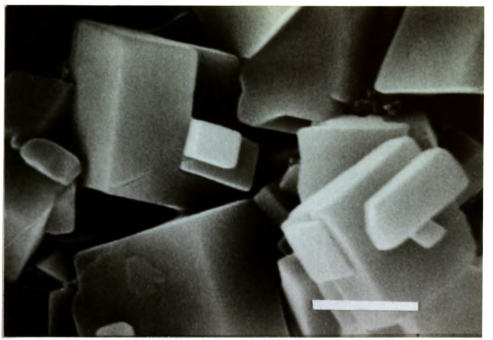

Figure 22

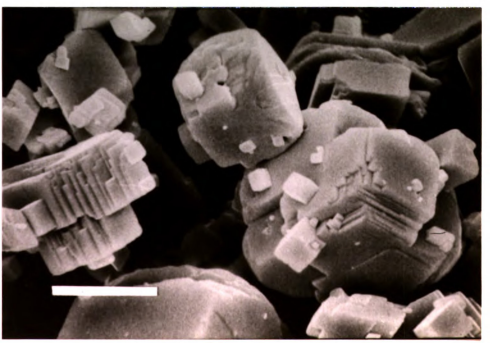

Figure 23

highly stepped surfaces (Fig. 23). It is consistent with dissolution and nucleation rate modelling (Morse, 1983; Berner, 1980) that rapid dolomitization of the coarse calcite resulted from its rough surface topography, causing rapid dissolution and/or providing more potential nucleation sites. Conversely, the extreme surface smoothness of the finer calcite provided fewer reactive sites, thus accounting for its slower reaction rate.

The compositions of dolomite produced early in the reactions may have also been related to substrate dissolution rates. The earliest dolomite on aragonite contained 61.5 mole % $CaCO_3$ in contrast to a value of 52.3 mole % $CaCO_3$ for HMC substrates. Rapid dissolution of aragonite may have reduced the Mg^{2+}/Ca^{2+} in solution, relative to the slowly dissolving HMC, directly effecting the degree of non-stoichiometry of the earliest dolomite crystals.

By the time the reactants had been completely replaced however, the dolomite had attained a rather uniform, near-stoichiometric composition. The relationship between dolomite non-stoichiometry and substrate mineralogy therefore appeared to be a relatively short-lived feature of the overall process.

Growth of Dolomite

Overall replacement rates did not depend specifically on the growth rate of dolomite crystals. The growth rate

of dolomite appeared to be rapid and similar for all mineralogies, once precipitation was initiated. Variation in the replacement rates were consequently a result of the differing lengths of time required for dolomite to nucleate on the various reactants.

A change in calcite dissolution textures accompanied the rapid growth of dolomite. It is suggested that the rate of calcite dissolution prior to dolomite precipitation was limited by a slow surface process, in accordance with the lattice-related etch features seen during that stage (see Fig. 7). As the concentration of the carbonate ion gradually increased via calcite dissolution, nucleation of dolomite ensued. A greater degree of disequilibrium with calcite could have then occurred locally as CO_3^{2-} and Ca^{2+} were quickly removed from solution by the growing dolomite. Dissolution of calcite could then proceed rapidly to produce rounded shapes.

APPLICATION OF EXPERIMENTAL RESULTS

Rock Selectivity

Experimental results suggest the importance of surface area variation in determining a reactant's susceptibility to dolomitization, despite the inverse relation exhibited

by the synthetic calcites (Fig. 21). Murray and Lucia (1967) present a case where dolomite of the Turner Valley Fm. (Mississippian) is concentrated in wackestone facies and occurs very sparsely in the grainstones. Dolomite within the wackestones shows a strong preference for selectivity of the mud matrix. It is consistent with the experimental results of the present study that this distribution, and others like it (for example, Armstrong et al, 1980), could be a consequence of rapid dissolution in the mud supported sediments. Locally high aCO_3^{2-} would then favor their replacement over the coarse grained fractions of the same rock.

Sibley (1980, 1982) reports selective dolomitization that post-dated fresh water diagenesis of forereef deposits of the Seroe Domi Fm. (Pliocene). Red algae were inferred to have recrystallized from primary HMC to LMC during fresh water diagenesis and were later dolomitized, but LMC spar cement that precipitated during the same fresh water episode resisted dolomitization. In this example, LMC red algae dissolved and dolomitized more rapidly than sparry calcite because of the presumed higher surface area of these allochems.

Carbonate Ion and Dolomitization

Accelerated reaction rates which resulted from the addition of Na_2CO_3 indicates the potential importance of the aCO_3^{2-} to dolomitization in natural diagenetic

settings. Small quantities of protodolomite have been found in unconsolidated Recent sediments within the fresh water/brackish zones below tidal flat hammocks of Andros Island (Gebelein et al, 1980). A characteristic of this setting is high carbonate alkalinity, about five times that of normal marine water. The pCO_2 is also about one-hundred times that of normal atmospheric conditions. Dolomite is not detected in the sediments exposed to normal sea water that surrounds the brackish zones.

Rapid dissolution and precipitation of aragonite within the needle mud sediment occurs on a seasonal basis. The dolomite contains 56-62 mole % $CaCO_3$, very similar in composition to the initial, rapidly precipitated dolomites produced in the aragonite experiments of this study. It does not occur as a replacement product however, but as a cement. High carbonate alkalinity and rapid reaction rates, associated with the spatial distribution of this example of Recent dolomite, suggest a natural analog to the experimental results of the present study.

Holocene diagenesis of late Pleistocne rocks (Falmouth Fm.) in the mixing zone beneath Jamaica represents another setting where high aCO_3^{2-} may promote early, near-surface dolomitization. Meteoric waters on Jamaica are grossly oversaturated with calcite due to extremely high pCO_2 (Land, 1973a) and should therefore have high carbonate alkalinity. Mixtures of these waters with moderate amounts of sea water are oversaturated with

dolomite (Land, 1973a).

Diagenesis in the Jamaican meteoric phreatic zone includes conversion of HMC to LMC, partial aragonite dissolution and precipitation of calcite cement. Mineralogical alteration of the primary sediment is absent in the marine phreatic zone. Partial dolomitization of HMC micrite and red algae is found to occur in the mixing zone between the meteoric and marine phreatic zones (Land, 1973b). The supply of abundant carbonate from meteoric waters and Mg^{2+} from sea water may create a solution particulatly favorable for dolomitization.

SUMMARY AND CONCLUSIONS

Important results pertaining to the origins of sedimentary dolomite are:

1) Selective dolomitization cannot be explained simply in terms of either surface area or mineralogical variation. Reactant surface properties (determined qualitatively from SEM and light microscopy) are suggested to have made a significant contribution to reaction rates. A fine grained, very smooth-surfaced calcite was far more resistant to dolomitization than both a coarser grained but rough-surfaced reagent calcite and a crushed (and presumably strained) Iceland spar calcite, also of lesser

surface area. Among samples sharing identical preparatory procedures, an apparent mineralogical effect on dolomitization susceptibility was recognized: aragonite dolomitized more rapidly than Iceland spar calcite which dolomitized more rapidly than HMC (12 mole % $MgCO_3$).

2) An interval of partial substrate dissolution, as a source of CO_3^{2-}, preceded the first appearance of dolomite. This interval was typically much longer than the time between the first appearance of dolomite and 100% replacement. Variation in the replacement rates arose as a function of the different lengths of time required for dolomite to nucleate on the various reactants.

3) Addition of sodium carbonate beyond calcite saturation accelerated the replacement rate by reducing the time interval preceding the first detection of dolomite. The activity of CO_3^{2-} at the time of dolomite nucleation is unknown.

4) SEM revealed that the most rapidly dolomitized substrate (excluding external CO_3^{2-} runs) also dissolved most rapidly prior to the first appearance of dolomite, and vice versa. It is suggested that aCO_3^{2-} is important in the process of selective dolomite nucleation and may be directly related to the relative rates of substrate dissolution.

5) The final dolomite composition was slightly Ca-rich (average equals 51.7 mole % $CaCO_3$) and uniform between reactants. More pronounced dolomite non-stoichiometry occurred very early on in the reaction sequence. Each reactant mineralogy was characterized by a distinct early-dolomite compositional range that appeared to be related to the composition and/or dissolution rate of the reactant.

6) Dolomite crystal seeding produced no rate change.

APPENDIX

APPENDIX

Experimental Results

Reactant Reagent calcite, Sample CF2

Runs 1-7
Reaction time 38-200 hrs.
Products and description Dissolution of substrate is evident in later runs , otherwise unaltered from starting material.

Run 8
Reaction time 224 hrs.
Products and description 100% dolomite; 50.9 mole % $CaCO_3$; euhedral rhombs; ordering is fair.

Run 9
Reaction time 224 hrs.
Products and description Approx. 50% calcite and 50% dolomite; dolomite is disordered with 57.7 mole % $CaCO_3$; magnesite is present, 15 mole % $CaCO_3$.

Run 10
Reaction time 257.5 hrs.
Products and description 100% dolomite with 50.6 mole % $CaCO_3$; strong, well defined ordering peaks; euhedral rhombs of both limpid and highly porous varieties (from SEM); no magnesite.

Run 11
Reaction time 264 hrs.
Products and description 100% dolomite with 51.0 mole % $CaCO_3$;well defined order peaks; dolomite is slightly coarser than reactant grains; limpid and clouded varieties present; no magnesite.

Run 12
Reaction time 308 hrs.
Products and description 100% dolomite; 50.0 mole % $CaCO_3$; well-ordered; euhedral.

Reactant Reagent calcite, Sample CI2

Runs 1-3
Reaction time 30-100 hrs.
Products and description No changes observed

Run 4
Reaction time 120 hrs.
Products and description 100% dolomite with 51.5 mole % $CaCO_3$; euhedral rhombs; well defined order peaks; no magnesite.

Run 5
Reaction time 130 hrs.
Products and description 100% dolomite with 51.3 mole % $CaCO_3$; well-ordered.

Run 6
Reaction time 180 hrs.
Products and description 100% dolomite with 51 mole % $CaCO_3$; unit extinguishing interiors of rhombs; rough surfaces; no magnesite; well-ordered.

Reactant Synthetic calcite, Sample CI3

Run 1
Reaction time 149 hrs.
Products and description 100 % dolomite with 50.6 mole % $CaCO_3$; cloudy rhombs; sub-euhedral; ordering is fair.

Run 2
Reaction time 135 hrs.
Products and description Approx. 100% calcite reactant; sparsely distributed magnesite, 12 mole % $CaCO_3$.

Reactant Iceland spar calcite, Sample CC

Runs 1-2
Reaction time 15 and 37 hrs.
Products and description No visible change with SEM.

Run 3
Reaction time 65 hrs.
Products and description Approx. 100% calcite reactant; very fine (<2μm) magnesite along cleavage traces and steps.

Runs 4 and 5
Reaction time 80 and 100 hrs.
Products and description Approx. 100% calcite reactant; minor magnesite with 14.5 and 13 mole % $CaCO_3$.

Run 6 and 7
Reaction time 125 and 200 hrs.
Products and description Approx. 100% reactant; magnesite is commonly aligned along twin planes on substrate.

Run 8
Reaction time 240 hrs.
Products and description 100% dolomite with 51.4 mole % $CaCO_3$; fairly well-ordered; unit extinguishing grain interiors; rough surface texture; crude pseudomorphs after primary grain.

Run 9
Reaction time 220 hrs.
Products and description Approx. 100% calcite reactant.

Run 10
Reaction time 220 hrs.
Products and description 100% dolomite; texturally identical to Run 8; 52 mole % $CaCO_3$.

Run 11
Reaction time 239 hrs.
Products and description 95% calcite and 5% dolomite; dolomite has 52 mole % $CaCO_3$; very diffuse, weak major peak; abundant magnesite, 11.7 mole % $CaCO_3$.

Run 12
Reaction time 240 hrs.
Products and description Approx. 100% calcite reactant with magnesite; obvious dissolution of substrate.

Run 13 and 14
Reaction time 269 hrs.
Products and description 100% dolomite with 50 mole % $CaCO_3$; well-ordered; rough grain surfaces with unit extinguishing cores; no magnesite.

Run 15
Reaction time 360 hrs.
Products and description 100% dolomite; 51.2 mole % $CaCO_3$; well-ordered; product grains are composed of an assembledge of uniformly aligned crystals; highly stepped surfaces and unit extinction are characteristic.

Reactant Iceland spar calcite, Sample CI

Runs 1 and 2
Reaction time 80 hrs.
Products and description Approx. 100% calcite reactant; sparse magnesite with 9.4 mole % $CaCO_3$; etching of substrate is pervasive.

Run 3
Reaction time 130 hrs.
Products and description 60% calcite reactant and 40% dolomite; dolomite is disordered with 54 mole % $CaCO_3$; calcite grains are rounded by dissolution.

Run 4
Reaction time 150 hrs.
Products and description 100% dolomite; limpid, euhedral rhombs; 55 mole % $CaCO_3$; ordering is fair.

Run 5
Reaction time 80 hrs.
Products and description Approx. 100% calcite reactant; etch features common; minor calcian magnesite with 13 mole % $CaCO_3$.

Run 6, 0.035 g Na_2CO_3 added
Reaction time 80 hrs.
Products and description Calcite just at X-ray detection limit; 95% dolomite with 50.9 mole % $CaCO_3$; well-ordered; non-undulatory ,unit extinction.

Run 7
Reaction time 145 hrs.
Products and description 100% dolomite; well-ordered; 52.2 mole % $CaCO_3$.

Run 8
Reaction time 160 hrs.
Products and description 100% dolomite; 52.2 mole % $CaCO_3$; fair ordering; rough surfaces; unit extinguishing cores; no magnesite.

Reactant Iceland spar calcite, sample CF

Runs 1-4
Reaction time 21-44 hrs.
Products and description Unchanged

Run 5
Reaction time 67.5 hrs.
Products and description 100% dolomite; 50.8 mole % $CaCO_3$; sub-euhedral, individual rhombs; hollowing of coarser grains is common; no magnesite.

Run 6
Reaction time 71 hrs.
Products and description 100% dolomite; 53 mole% $CaCO_3$; poorly-ordered.

Reactant HMC, sample HC

Run 1
Reaction time 176 hrs.
Products and description Approx. 100% HMC reactant; minor magnesite; randomly oriented; 12 mole % $CaCO_3$; minor dissolution evident.

Run 2
Reaction time 190 hrs.
Products and description Partial replacement by dolomite; approx. 30% dolomite; strong preferential alignment; 53.4 mole % $CaCO_3$; minor magnesite with 11.4 mole % $CaCO_3$.

Run 3
Reaction time 200 hrs.
Products and description Approx. 100% HMC; abundant magnesite; 11.1 mole % $CaCO_3$.

Run 4
Reaction time 208.5 hrs.
Products and description Approx. 100% dolomite with 51.2 mole % $CaCO_3$; poorly-ordered; rhombic outlines of originally rounded grains; unit extinction is observed; magnesite with 10.3 mole % $CaCO_3$ present.

Run 5
Reaction time 210.5 hrs.
Products and description 100% dolomite; 52.5 mole % $CaCO_3$; poorly-ordered; texture same as Run 4.

Run 6
Reaction time 216 hrs.
Products and description Approx. 100% dolomite; 53.4 mole % $CaCO_3$; poorly-ordered; trace magnesite.

Run 7
Reaction time 224 hrs.
Products and description 100% dolomite; 53 mole % $CaCO_3$; fair ordering.

Reactant HMC, sample HI

Run 1
Reaction time 190 hrs
Products and description Approx. 100% HMC reactant; sparse magnesite; 11.1 mole % $CaCO_3$.

Run 2
Reaction time 202 hrs.
Products and description Approx. 100% dolomite; 55.3 mole % $CaCO_3$; fair ordering; unit extinction is common excepting in cryptocrystalline areas, where the primary texture is inferred to have been cryptocrystalline.

Run 3
Reaction time 212 hrs.
Products and description Approx. 20% HMC reactant; 80% dolomite; 50.3 mole % $CaCO_3$; poorly-ordered; minor magnesite; 10.8 mole % $CaCO_3$

Run 4
Reaction time 218 hrs.
Products and description 100% dolomite; 53.7 mole % $CaCO_3$; fair to poor ordering; grain surfaces are rhombic shaped.

Reactant HMC, sample HF

Run 1
Reaction time 77 hrs.
Products and description Approx. 100% HMC reactant; trace magnesite with 11.4 mole % $CaCO_3$; rare dissolution features.

Run 2
Reaction time 92 hrs.
Products and description No visible change with SEM; very rare magnesite present.

Run 3
Reaction time 125 hrs.
Products and description Approx. 100% HMC reactant; rare magnesite crystals, $< 5\mu m$; HMC composition is identical to initial reactant.

Run 4
Reaction time 160 hrs.
Products and dsecription Approx. 100% dolomite, 50.3 mole % $CaCO_3$, well-ordered; coarse grains appear as polycrystalline assembledges, fines appear as monocrystalline grains, unit extinction prevalent; no distinct rhombic shapes with light microscope; minor magnesite, 10.8 mole % $CaCO_3$.

Run 5
Reaction time 169.5 hrs.
Products and description Approx. 50% HMC reactant and 50% dolomite with 50 mole % $CaCO_3$; disordered; faint rhombic overgrowths observed with light microscope; grains appear limpid; HMC composition same as original.

Run 6
Reaction time 186 hrs.
Products and description 100% dolomite, 50.6 mole % $CaCO_3$, rather poor ordering, grains are subhedral and limpid with faint rhombic outlines; minor magnesite with 9.7 mole % $CaCO_3$.

Run 7
Reaction time 190 hrs.
Products and description 100% dolomite, 50.3 mole % $CaCO_3$, fair ordering, limpid crystals very common.

Run 8
Reaction time 258.5 hrs.
Products and description 100% dolomite with 51.8 mole % $CaCO_3$, well-ordered, product retains original grain shapes with some addition of rhombic overgrowth.

Reactant Ward's Aragonite, Samole AC

Run 1
Reaction time 37 hrs.
Products and description 100% reactant; dissolution etching observed.

Run 2 and 3
Reaction time 75.5 and 84.5 hrs.
Products and description Approx. 100% reactant, strongly etched; new material is common but not X-ray detected.

Run 4
Reaction time 88 hrs.
Products and description Approx. 80% aragontie and 20% dolomite; dolomite has 63 mole % $CaCO_3$, disordered, euhedral rhombs, < 5um, see Figure 16.

Run 5-7
Reaction time 92, 98 and 100 hrs.
Products and description Approx. 100% aragontie; abundant clusters (< 2 m) of spherulitic material on the aragonite surface, not X-ray detected; this material strongly resembles amorphous products from room temperature experiments with Mg and Ca chloride solutions and high Mg/Ca ratios.

Run 8
Reaction time 104.5 hrs.
Products and description 50% aragonite and 50% dolomite with 58.9 mole % $CaCO_3$, poorly-ordered, dense mosaic of interlocking euhedral rhombs about 5μm in size.

Run 9
Reaction time 112 hrs.
Products and description 100% dolomite, 52.1 mole % $CaCO_3$, fair to poor ordering, texture identical to Run 8.

Reactant Ward's aragonite, Sample AI2

Run 1
Reaction time 55 hrs.
Products and description Approx. 100% aragonite reactant; abundant crystals on the aragonite surfaces which are not X-ray detected, crystal size is about 5-10μm.

Run 2
Reaction time 60 hrs.
Products and description 80% aragonite and 20% dolomite; diffuse and weak dolomite X-ray peak, limpid euhedral rhombs, 5μm in size, randomly oriented.

Run 3
Reaction time 68 hrs.
Products and description 100% dolomite, well-ordered, 51.1 mole % $CaCO_3$, dense mosaics of interlocking euhedral limpid rhombs, 5 m diameters.

Run 4
Reaction time 69 hrs.
Products and description 100% dolomite, well-ordered, 51 mole % $CaCO_3$, texturally identical to Run 3.

Reactant Ward's aragonite, Sample AI

Run 1 and 2
Reaction time 19 hrs.
Products and description 100% aragonite, unaltered.

Run 3
Reaction time 25 hrs.
Products and description Approx. 100% aragonite with abundant amorphous intermediate product.

Run 4
Reaction time 36 hrs.
Products and description 100% dolomite, 52 mole % $CaCO_3$, fair ordering, euhedral rhombs.

Run 5
Reaction time 34 hrs.
Products and description Identical to Run 3.

Run 6
Reaction time 46 hrs.
Products and description 100% dolomite, 62 mole % $CaCO_3$, disordered, euhedral rhombs with random orientation.

Run 7
Reaction time 55 hrs.
Products and description 100% dolomite with 51.4 mole % $CaCO_3$, fair ordering.

Run 8
Reaction time 63.5 hrs.
Products and description 100% dolomite with 50.9 mole % $CaCO_3$, well-ordered, texturally identical to Run 6.

Reactant Ward's Aragonite, Sample AF

Run 1
Reaction time 15 hrs.
Products and description Approximately 80-90% aragonite and 20-10% disordered dolomite with 60 mole % $CaCO_3$.

Run 2
Reaction time 20 hrs.
Products and description 100% aragonite with minor amorphous material.

Run 3
Reaction time 24.5 hrs.
Products and description 100% dolomite with 52.5 mole % $CaCO_3$, poorly-ordered, euhedral rhombs, no precursor texture preserved .

Run 4
Reaction time 27 hrs.
Products and description 100% dolomite with 51.7 mole % $CaCO_3$, fair ordering.

Reactant Synthetic Aragonite Needles, Sample AF2

Run 1 and 2
Reaction time 11 and 13.5 hrs.
Products and description Approx. 100% aragonite; rare prismatic crystals of a phase which escapes X-ray detection.

Run 3
Reaction time 16 hrs.
Products and description Dolomite with 64.3 mole % $CaCO_3$, disordered, euhedral rhombs about 5 m in size; HMC with 14 mole % $MgCO_3$ occurs sparsely as 15 m long euhedral, sharply terminated prisms; dolomite content >> HMC.

Run 4 and 5
Reaction time 17 and 24 hrs.
Products and description Identical to Run 2.

Run 6
Reaction time 37 hrs.
Products and description Dolomite with 62 mole % $CaCO_3$, poorly-ordered, euhedral 10 m rhombs; HMC with 16.2 mole % $MgCO_3$, rhombic shaped; dolomite content >> HMC.

Run 7
Reaction time 50 hrs.
Products and description 100% dolomite with 52.6 mole % $CaCO_3$, fairly well-ordered, individual euhedral rhombs, crystal size (5μm) is finer than HMC intermediates (15μm) detected in earlier runs.

Results of External Carbonate and Seeding

Reactant Iceland Spar Calcite, Sample CF'

Run Ca
Reaction time 24 hrs.
Additive 0.0175 gram seeds, ordered, near-stoichiometric dolomite
Result LMC and magnesite, excluding seeds.

Run Cb
Reaction time 24 hrs.
Additive 0.035 gram Na_2CO_3
Result LMC plus minor magnesite.

Run Cc
Reaction time 35 hrs.
Additive 0.035 gram Na_2CO_3
Result 15% disordered dolomite, 59 mole % $CaCO_3$; 85% LMC.

Run Cd
Reaction time 35 hrs.
Additive 0.0175 gram seeds, ordered, near-stoichiometric dolomite
Result 100% LMC, excluding seeds.

Run Ce
Reaction time 47.5 hrs.
Additive 0.0175 gram seeds, ordered, near-stoichiometric dolomite
Result 100% LMC, excluding seeds.

Run Cf
Reaction time 47.5 hrs.
Additive 0.035 gram Na_2CO_3
Result 80% dolomite, poorly-ordered, 52.2 mole % $CaCO_3$; 20% LMC.

Run Cg
Reaction time 60 hrs.
Additive 0.035 gram Na_2CO_3
Result 85% dolomite with 55 mole % $CaCO_3$; 15% LMC.

Run Ch
Reaction time 60 hrs.
Additive 0.035 gram dolomite seeds, ordered, near-stoichiometric
Result 100% LMC, excluding seeds.

Run Ci
Reaction time 60 hrs.
Additive Control
Result 100% LMC

Run Cj
Reaction time 75 hrs
Additive 0.0175 gram seeds, ordered, near-stoichiometric dolomite
Result 100% dolomite, poorly-ordered, 52.2 mole % $CaCO_3$.

Run Ck
Reaction time 75 hrs.
Additive Control
Result 50% disordered dolomite, 56.8 mole % $CaCO_3$; 50% LMC.

Reactant Ward's Aragonite, Sample AI

Run Ae
Reaction time 10.5 hrs
Additive 0.035 gram Na_2CO_3
Result 20% disordered dolomite with 61.5 mole % $CaCO_3$; 80% aragonite.

Run Af
Reaction time 10.5 hrs.
Additive 0.0175 gram seeds, ordered, near-stoichiometric dolomite
Result 100% aragonite

Run Ab
Reaction time 15 hrs.
Additive 0.035 gram Na_2CO_3
Result 50% disordered dolomite with 60.8 mole % $CaCO_3$; 50% aragonite.

Run Ag
Reaction time 17 hrs.
Additive 0.0175 gram dolomite seeds, disordered, 62 mole % $CaCO_3$
Result 100% aragonite.

Run Ah
Reaction time 17 hrs.
Additive 0.035 gram Na_2CO_3
Result 90% dolomite, 64.6 mole % $CaCO_3$, disordered; 10% HMC with 9.5 mole % $MgCO_3$.

Run Ad
Reaction time 20 hrs.
Additive 0.035 gram Na_2CO_3
Result 75% dolomite with 59.9 mole % $CaCO_3$; 25% aragonite.

Run Ac
Reaction time 20 hrs.
Additive Control

Result 12% disordered dolomite with 61.5 mole % $CaCO_3$; 88% aragonite.

Run Aa
Reaction time 20 hrs.
Additive 0.0175 gram seeds, ordered, near-stoichiometric dolomite
Result 30% dolomite, 54 mole % $CaCO_3$; 70% aragonite.

Run Ai
Reaction time 32 hrs.
Additive Control
Result 100% dolomite with 63 mole % $CaCO_3$, disordered.

Run Aj
Reaction time 32 hrs.
Additive 0.0175 gram seeds, ordered, near-stoichiometric dolomite
Result 100% dolomite with 63 mole % $CaCO_3$, disordered.

BIBLIOGRAPHY

BIBLIOGRAPHY

Adamson, A.W., 1982, Physical Chemistry of Surfaces: New York, John Wiley and Sons, Inc., 664p.

Armstrong, A.K., Snavely, P.D. Jr. and Addicot, W.O., 1980, Porosity evolution of Upper Miocene reefs, Almeria Province, southern Spain: Am. Assoc. Petroleum Geologists Bull., v. 64, no. 2, p. 188-208.

Badiozamani, K., 1973, The Dorag dolomitization model - application to the Middle Ordovician of Wisconsin: Jour. Sed. Pet., v. 43, no. 4, p. 965-984.

Baker, P.A. and Kastner, M., 1981, Constraints on the formation of sedimentary dolomite: Science, v. 213, p. 214-216.

Bathurst, R.C., 1975, Carbonate Sediments and their Diagenesis: Developments in Sedimentology, 12, New York, Elsevier, 658p.

Berner, R.A., 1980, Early diagenesis: Princeton Univ. Press, 241p.

Buchbinder, B., 1979, Facies and environments of Miocene reef limestones in Israel: Jour. Sed. Pet., v. 49, no. 4, p. 1323-1344.

Bullen, S.B., 1983, Synthetic dolomite textures: Unpublished Masters Thesis, Michigan State Univ., 152p.

Carlson, W.D., 1983, The polymorphs of $CaCO_3$ and the aragonite-calcite transformation: in, Reviews in Mineralogy, v. 11, chap. 6, pp. 191-225, Mineralogical Society of America.

Carpenter, A.B., 1980, The chemistry of dolomite formation I: the stability of dolomite: in, Zenger, D.H., Dunham, J.B., and Ethington, R.L., eds., Concepts and Models of Dolomitization: Soc. Econ. Paleontologists Mineralogists Spec. Pub. 28, p. 111-122.

Folk, R.L. and Land, L.S., 1975, Mg/Ca ratio and salinity: two controls over crystallization of dolomite: Am. Assoc. Petroleum Geologists Bull., v. 59, no. 1, p. 60-68.

Gaines, A.M., 1980, Dolomitization kinetics: recent experimental studies: in, Zenger, D.H., Dunham, J.B., and Ethington, R.L., eds., Concepts and Models of Dolomitization: Soc. Econ. Paleontologists Mineralogists Spec. Pub. 28, p. 81-86.

Graf, D.L., and Goldsmith, J.R., 1956, Some hydrothermal syntheses of dolomite and protodolomite: Jour. of Geology, v. 64, p. 173-186.

Grethen, B.L., 1979, The synthesis of dolomite at 150C: Unpublished M.S., University of Missouri, 81p.

Gudramovics, R., 1981, A geochemical and hydrological investigation of a modern coastal marine sabkha: Unpublished M.S., Michigan State University, 107p.

Katz, A. and Matthews, A., 1977, The dolomitization of $CaCO_3$: an experimental study at 252-295C: Geochimica et Cosmochimica Acta, v. 41, p. 297-308.

Kocurko, J.M., 1979, Dolomitization by spray-zone brine seepage, San Andres, Coloumbia: Jour. Sed. Pet., v. 49, no. 1, p. 209-214.

Land, L.S., 1967, Diagenesis of skeletal carbonates: Jour. Sed Pet., v. 37, no. 3, p. 914-930.

Land, L.S. and Epstein, S., 1970, Late Pleistocene diagenesis and dolomitization, North Jamaica: Sedimentology, v. 14, p. 187-200.

Land, L.S., 1973a, Contemporaneous dolomitization of middle Pleistocene reefs by meteoric water, North Jamaica: Bull. Mar. Sci., v. 23, p. 64-92.

Land, L.S., 1973b, Holocene meteoric dolomitization of Pleistocene limestones, North Jamaica: Sedimentology, v. 20, p. 411-424.

Lippmann, F., 1973, Sedimentary Carbonate Minerals: Springer-Verlag, New York, 228p.

Morrow, D.W., 1982, Diagenesis 1; Dolomite, Part 1: Geoscience Canada, v. 9, no. 1, p. 5-13.

Morse, J.W., 1983, The kinetics of calcium carbonate dissolution and precipitation: in, Reviews in Mineralogy, v. 11, Chap. 7, p. 227-264, Mineralogical Society of America.

Murray, R.C. and Lucia, F.J., 1967, Cause and control of dolomite distribution by rock selectivity: Geol. Soc. Am. Bull. 78, pt. 1, p. 21-35.

Nechiporenko, G.O. and Bondarenko, G.P., 1984, Experimental data on conditions of formation of a series of magnesian calcites: International Geology Review, v. 26, p. 189-197.

Oomori, T., Kiyoshi, K., Taira, T. and Kitano, Y., 1983, Syntheitc studies of protodolomite from brine waters: Geochemical Journal, v. 17, p. 147-152.

Rosenberg, P.E. and Holland, H.D., 1964, Calcite-dolomite-magnesite stabiltiy relations in solutions at elevated temperatures: Science, v. 145, p. 700-701.

Saller, A.H., 1984, Petrologic and geochemical constraints on subsurface dolomite, Enewetak Atoll: an example of dolomitization by normal seawater: Geology, v. 12, p. 217-220.

Schmidt, V., 1965, Facies, diagenesis, and related reservoir properties in the Gigas Beds (Upper Jurassic), northwestern Germany: in, Pray, L.C. and Murray, R.C., eds., Dolomitization and Limestone Diagenesis: Soc. Econ. Paleontologists Mineralogists Spec. Pub. 13, p. 124-169.

Schofield, J.C. and Nelson, C.S., 1978, Dolomitization and Quaternary climate of Niue Island, Pacific Ocean: Pacific Geology 13, p. 37-48.

Schlanger, S.O., 1957, Dolomite growth in coralline algae: Jour. Sed. Pet., v. 27, p. 181-186.

Sibley, D.F., 1980, Climatic control of dolomitization, Seroe Domi Fm. (Pliocene), Bonaire, N.A.: in, Zenger, D.H., Dunham, J.B., and Ethington, R.L., eds., Concepts and Models of Dolomitization: Soc. Econ. Paleontologists Mineralogists Spec. Pub. 28, p. 247-258.

Sibley, D.F., 1982, The origin of common dolomite fabrics: clues from the Pliocene: Jour. Sed. Pet., v. 52, no. 4, p. 1087-1100.